Fast NMDA Receptor–Mediated Synaptic Currents in Neurons From Mice Lacking the ε2 (NR2B) Subunit

Kenneth R. Tovar, Kathleen Sprouffske and Gary L. Westbrook

J Neurophysiol 83:616-620, 2000.

Journal of Neurophysiology publishes original articles on the function of the nervous system. It is published 12 times a year (monthly) by the American Physiological Society, 9650 Rockville Pike, Bethesda MD 20814-3991. ISSN: 0022-3077, ESSN: 1522-1598. Visit our website at http://www.the-aps.org/.

Fast NMDA Receptor–Mediated Synaptic Currents in Neurons From Mice Lacking the ε2 (NR2B) Subunit

KENNETH R. TOVAR, KATHLEEN SPROUFFSKE, AND GARY L. WESTBROOK
Vollum Institute, Oregon Health Sciences University, Portland, Oregon 97201-3098

Tovar, Kenneth R., Kathleen Sprouffske, and Gary L. Westbrook. Fast NMDA receptor–mediated synaptic currents in neurons from mice lacking the ε2 (NR2B) subunit. *J. Neurophysiol.* 83: 616–620, 2000. The *N*-methyl-D-aspartate (NMDA) receptor has been implicated in the formation of synaptic connections. To investigate the role of the ε2 (NR2B) NMDA receptor subunit, which is prominently expressed during early development, we used neurons from mice lacking this subunit. Although $\epsilon2^{-/-}$ mice die soon after birth, we examined whether NMDA receptor targeting to the postsynaptic membrane was dependent on the ε2 subunit by rescuing hippocampal neurons from these mice and studying them in autaptic cultures. In voltage-clamp recordings, excitatory postsynaptic currents (EPSCs) from $\epsilon2^{-/-}$ neurons expressed an NMDA receptor–mediated EPSC that was apparent as soon as synaptic activity developed. However, compared with wild-type neurons, NMDA receptor–mediated EPSC deactivation kinetics were much faster and were less sensitive to glycine, but were blocked by Mg^{2+} or AP5. Whole cell currents from $\epsilon2^{-/-}$ neurons were also more sensitive to block by low concentrations of Zn^{2+} and much less sensitive to the ε2-specific antagonist ifenprodil than wild-type currents. The rapid NMDA receptor–mediated EPSC deactivation kinetics and the pharmacological profile from $\epsilon2^{-/-}$ neurons are consistent with the expression of ζ1/ε1 diheteromeric receptors in excitatory hippocampal neurons from mice lacking the ε2 subunit. Thus ε1 can substitute for the ε2 subunit at synapses and ε2 is not required for targeting of NMDA receptors to the postsynaptic membrane.

INTRODUCTION

N-methyl-D-aspartate (NMDA) receptors are composed of two subunit types, ζ and ε (or NR1 and NR2 in the rat). In the hippocampus, ε1 and ε2 are the predominantly expressed ε subunits in excitatory neurons (Monyer et al. 1994; but see Das et al. 1998). Mice lacking the ε2 subunit ($\epsilon2^{-/-}$) die soon after birth but can survive for a few days with hand feeding. Hippocampal slices obtained from these mice at postnatal day 3 lack a synaptic NMDA receptor–mediated component (Kutsuwada et al. 1996), indicating that early in development ε2-containing receptors are required either for formation of functional NMDA receptors or synaptic localization of receptors. Mice lacking the intracellular C-terminal domain of ε2 show a similar phenotype (Sprengel et al. 1998), providing further evidence for a role of the ε2 subunit in targeting to the postsynaptic density (PSD). In contrast, mice lacking the ε1 subunit are viable but have attenuated long-term potentiation (LTP) (Sakimura et al. 1995). The ε1 subunit is detected at very low levels in early development (Li et al. 1998; Monyer et al. 1994), but NMDA receptors containing the ε1 subunit are incorporated into the synaptic receptor complement soon after synapses have begun to form in vitro (Stocca and Vicini 1998; Tovar and Westbrook 1999). We now report that neurons cultured from $\epsilon2^{-/-}$ mice express NMDA receptor–mediated EPSCs with unusually rapid deactivation kinetics and distinctive pharmacological properties, consistent with expression of ζ1/ε1 diheteromeric receptors. Thus the ε2 subunit is not required for the formation of dual-component EPSCs. Likewise, incorporation of NMDA receptors at synapses can occur independently of the ε2 subunit.

The costs of publication of this article were defrayed in part by the payment of page charges. The article must therefore be hereby marked "*advertisement*" in accordance with 18 U.S.C. Section 1734 solely to indicate this fact.

METHODS

Breeding and cell culture

Because mice lacking both ε2 alleles die soon after birth, heterozygous ($\epsilon2^{+/-}$) mice in a C57BL/6 background were used for generating $\epsilon2^{-/-}$ mice. The heterozygous mouse colony was derived from $\epsilon2^{+/-}$ mice (Kutsuwada et al. 1996). Hippocampal neurons from neonatal $\epsilon2^{-/-}$ mice were rescued and grown in microisland cultures to examine the postsynaptic phenotype of $\epsilon2^{-/-}$ neurons. Litters from heterozygous matings delivered 19–19.5 days after mating plugs were detected and ranged from 5–11 pups. Because mice lacking the ε2 subunit are unable to nurse (Kutsuwada et al. 1996) and $\epsilon2^{+/-}$ mothers rarely nursed their pups, neurons from each newborn pup were cultured individually with tissue preserved for genotyping (see *Genotyping*). All cultures were done using newborn animals. As previously described (Bekkers and Stevens 1991) hippocampi from these animals were removed, enzymatically (papain; Collaborative Research) and mechanically dissociated and plated in microisland culture. The microisland substrate was prepared by spraying agarose-coated glass coverslips with polylysine and collagen. Neurons were plated at low density on this substrate to promote the formation of "autaptic" synapses. Excitatory postsynaptic currents (EPSCs) were apparent 6–7 days after plating.

Genotyping

All genotyping was done using polymerase chain reaction (PCR) amplification of genomic DNA prepared from mouse tissue. Tissue samples were incubated in proteinase K (0.5 mg/ml; GibcoBRL) at 55°C for ≥12 h. Samples were centrifuged and the supernatant was added to an equal volume of isopropanol to precipitate genomic DNA. The samples were spun again to pellet the DNA. The pellet was washed in ice cold 70% ethanol and allowed to dry. Genomic DNA was resuspended in TE buffer (10 mM Tris, 1 mM EDTA, pH 8.0) and added to the PCR mixture of each of two reactions. All samples were subjected to two separate reactions (see Fig. 1 for details). PCR analysis was done using *Taq* polymerase and Promega (Madison, WI) reagents. Reaction products were run on 2% agarose gels and visualized using ethidium bromide. Gel purification and sequencing of the

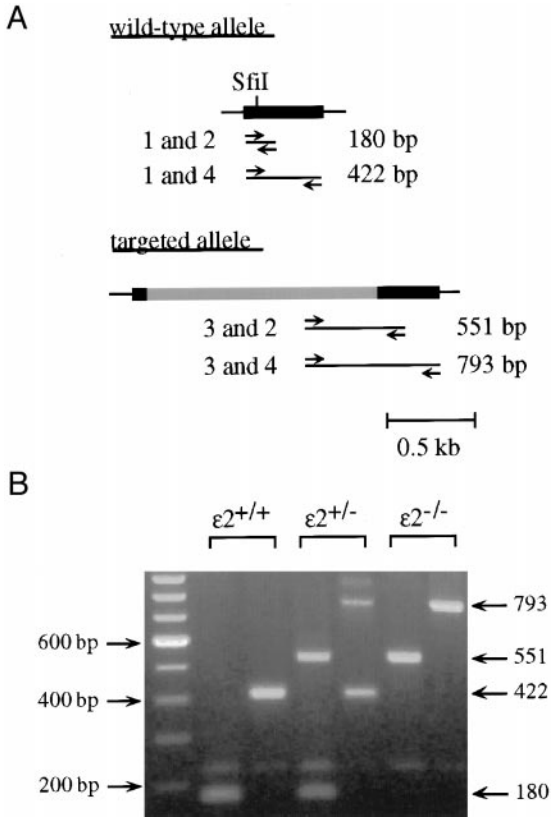

FIG. 1. Genotyping of $\epsilon 2$-targeted mice. Mice were genotyped using the polymerase chain reaction (PCR), allowing determination of the genotype of the animal within 2–3 days after plating. Two separate reactions were used for each genomic DNA sample. Primer orientation and placement is shown in *A*. Reactions differed only in the primers used (see METHODS). Because each reaction amplifies a product from wild-type and targeted alleles, every reaction will result in a product and thus acts as a control on the other reaction. Dark bar; targeted exon with the restriction site (*Sfi* I) into which the targeting vector (gray bar under "targeted allele") was inserted. Each animal was genotyped using two reactions, as shown in *B*. Reaction 1 contained primers 1, 2, and 3; Reaction 2 contained primers 1, 3, and 4.

reaction products yielded the expected DNA sequences (data not shown). Primer sequences were thus: *Primer 1*; 5′-ATgAAgCCCA gCgCAgAgTg-3′; *Primer 2*; 5′-ATggAAgTCAT CTTTCTCgTg-3′; *Primer 3*; 5′-ggCTACCTgC CCATTCgACC ACCAAgCgAA AC-3′; and *Primer 4*; 5′-AggACTCATC CTTATCTgCC ATTATCATAg-3′. The cycling conditions (Perkin-Elmer GeneAmp 2400, Foster City, CA) were 30 cycles of 94°C (melting) for 30 s, 67°C (annealing) for 40 s, and 72°C (extension) for 50 s. The reaction solution contained Mg^{2+} (2 mM), dNTPs (0.2 mM each), oligonucleotide primers (0.01 mg/ml each), *Taq* polymerase (2.5 units), reaction buffer (5 μL), and 2 μl of solubilized genomic DNA (50 μl final volume) in HPLC water. Each animal was genotyped using two reactions, as shown in Figure *1B*.

Electrophysiology

The extracellular recording solution contained (in mM) 168 NaCl, 2.4 KCl, 10 HEPES, 10 D-glucose, 0.2–2.6 $CaCl_2$, 0.01–0.02 glycine, 0.01 bicuculline methiodide (BMI), and 0.005 6-nitro-7-sulfamoyl-benzo[f]quinoxaline-2, 3-dione (NBQX) (325 mmol/kg final osmolality; pH 7.4) in HPLC-grade water. The intracellular recording solution contained (in mM) 150 K-gluconate, 1.418 $CaCl_2$, 2 $MgCl_2$, 10 EGTA, 10 HEPES, 2 Na_2ATP, and 0.2 GTP (320 mmol/kg final osmolality; pH 7.4). Recording electrodes (TW150F-6; World Precision Instruments, Sarasota FL) had resistances of 1–5 MΩ. Autaptic EPSCs were evoked using a depolarization (to +10 mV for 0.5 ms). Fast solution exchanges were made with quartz flow pipes mounted to a piezo-electric bimorph driven by a stimulus isolation unit (Winston Electronics, Palo Alto, CA). Flow pipes were placed 50–100 μm from the cell body. Recordings were done using an Axopatch 2C amplifier and pCLAMP acquisition software (Axon Instruments, Foster City, CA). Data were low-pass filtered at 2.5 kHz, collected at 5 kHz and, analyzed using Axograph (Axon Instruments). Data from dose-response experiments were fitted with $I = I_{max}/[1+(EC_{50}/A)^n]$, where I is the current response, I_{max} is the maximum response, A is the glycine concentration, and n is the Hill coefficient. Each concentration tested represents data from ≥4 neurons. For glycine and antagonist experiments, neurons were preequilibrated with the drug at the concentration being tested. Control (NMDA, 1 mM) and experimental responses (NMDA plus drug) were interleaved to control for possible run-down of the whole cell current. Whole cell current amplitudes were measured by averaging three points on either side of the absolute peak current. All data are reported as mean ± SE and were compared using an unpaired Student's *t*-test. All data are from neurons ≤10 days in vitro (DIV). Because the occurrence of wild-type and $\epsilon 2^{-/-}$ animals in the same litter was rare, data from wild-type neurons was obtained primarily from congenic animals rather than littermates of $\epsilon 2^{-/-}$ animals. All salts and drugs were from Sigma (St. Louis, MO) except for BMI, NBQX, NMDA, and ifenprodil (RBI, Natick, MA). Statistical comparisons were made using Student's *t*-test, with significance set at $P < 0.05$.

RESULTS

Genotyping $\epsilon 2$-targeted mice

Figure 1*A* shows the organization of $\epsilon 2$ wild-type and targeted alleles and the alignment of the PCR primers. The primers were designed to amplify the designated genomic DNA regions of wild-type and targeted alleles across insert/wild-type junctions. Two separate PCRs were used to determine the genotype of each animal. Each PCR was designed to amplify a different pair of reaction products (bracketed lanes in Fig. 1*B*). This resulted in a unique pair of reactions for $\epsilon 2^{+/+}$ and $\epsilon 2^{-/-}$ animals, whereas $\epsilon 2^{+/-}$ animals had four reaction products. Genotypes from progeny of heterozygous mice pairings were $22(^{+/+}):70(^{+/-}):24(^{-/-})$, not significantly different from a Mendelian distribution (using χ^2 criteria). Genotyping of outbred litters (resulting from $\epsilon 2^{+/-}$ and wild-type pairings) produced a wild-type to heterozygote ratio of 43:31, indicating that our genotyping method did not favor the production of reaction products from the targeted allele.

NMDA receptor–mediated EPSCs from $\epsilon 2^{-/-}$ neurons

EPSCs in wild-type hippocampal neurons have two kinetically distinct components. The fast component (deactivation τ: ca. 1–5 ms) results from the activation of AMPA receptors whereas the slow component (deactivation τ: ca. 40 and 300 ms) results from NMDA receptor activation (McBain and Mayer 1994). In $\epsilon 2^{-/-}$ neurons, EPSCs were apparent in microisland cultures after 6–7 days. However, the decay of the EPSC did not show two distinct kinetic components, characteristic of AMPA and NMDA receptor–mediated EPSCs in wild-type neurons. The NMDA receptor antagonist AP5 markedly shortened the decay of the dual-component EPSC in wild-type neurons (Fig. 2*A*) but had a much less profound effect on the decay in $\epsilon 2^{-/-}$ neurons (Fig. 2*B*). The AP5-sensitive components from wild-type and $\epsilon 2^{-/-}$ neurons are

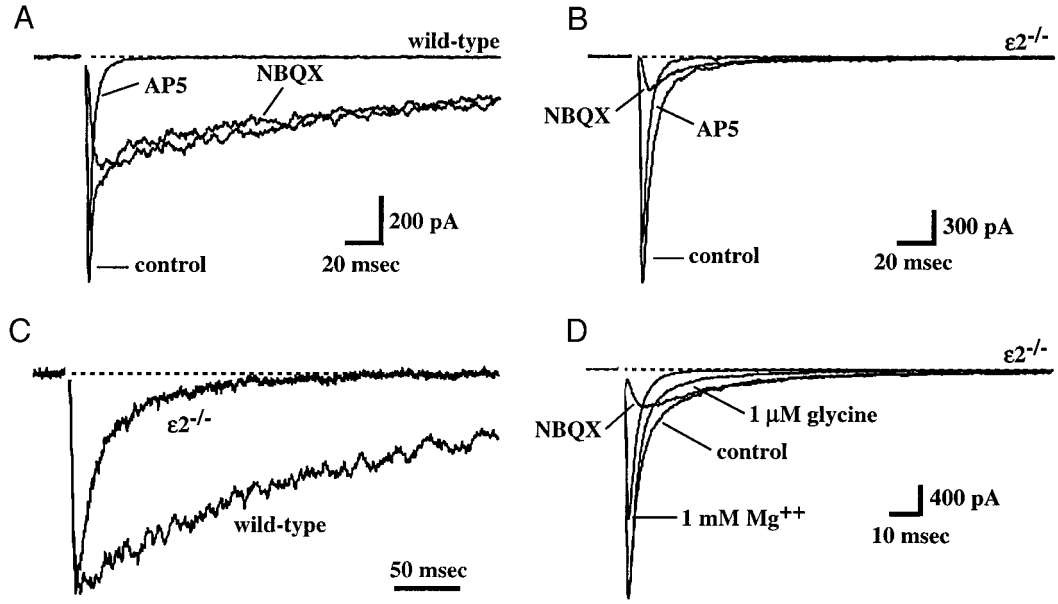

FIG. 2. Fast kinetics of *N*-methyl-D-aspartate (NMDA) receptor–mediated excitatory postsynaptic currents (EPSCs) in $\epsilon 2^{-/-}$ hippocampal neurons. EPSCs in wild-type (*A*) and $\epsilon 2^{-/-}$ (*B*) neurons show both 6-nitro-7-sulfamoylbenzo[f]quinoxaline-2, 3-dione (NBQX)- and AP5-sensitive currents. The AP5-sensitive currents are superimposed and normalized in *C*, showing that the deactivation kinetics of the AP5-sensitive current in *B* were much faster than the AP5-sensitive current in *A*. *D*: slow component of the EPSC is decreased by lowering the glycine concentration and completely blocked by 1 mM Mg^{2+} (NBQX-sensitive current is shown), characteristic of NMDA channels. The control, NBQX, and 1 mM Mg^{2+} currents were done in 10 μM glycine.

superimposed in Fig. 2*C*. The deactivation kinetics of NMDA receptor–mediated EPSCs from wild-type neurons (Fig. 2, *A* and *C*) were well-fitted with two exponentials ($\tau_f = 42.4 \pm 3.6$ ms; $\tau_s = 288.8 \pm 24.1$ ms, $n = 15$), similar to cultured rat neurons (e.g., Tovar and Westbrook 1999). In contrast, the deactivation kinetics of EPSCs from $\epsilon 2^{-/-}$ neurons (Fig. 2*B*) were dramatically faster ($\tau_f = 20.6 \pm 1.7$ ms; $\tau_s = 100.8 \pm 13.6$ ms, $n = 7$). For NMDA receptor–mediated EPSCs from $\epsilon 2^{-/-}$ neurons, the sum of squared errors (SSE) for two-exponential fits was 9.9 ± 3.4 times better than for a single exponential fit. In $\epsilon 2^{-/-}$ neurons, the deactivation kinetics were dominated by τ_f. The ratio (τ_f/τ_s) was 6.04 ± 1.09 ($n = 7$) for $\epsilon 2^{-/-}$ neurons and 1.16 ± 0.15 ($n = 15$) for wild-type neurons. Although the deactivation kinetics from $\epsilon 2^{-/-}$ neurons were usually well-fitted with two exponentials, in two cases the deactivation could be fitted with a single exponential ($t \approx 34$ ms). The fast deactivation kinetics of NMDA receptor–mediated EPSCs in $\epsilon 2^{-/-}$ neurons are consistent with deactivation kinetics expected of recombinant $\zeta 1/\epsilon 1$ diheteromeric receptors (Vicini et al. 1998) and are much faster than EPSC deactivations seen in other preparations (McBain and Mayer 1994; see however, Bardoni et al. 1998). Consistent with an NMDA receptor–mediated EPSC, currents from $\epsilon 2^{-/-}$ neurons became larger by increasing extracellular glycine ($n = 4$) and were completely blocked by Mg^{2+} ($n = 4$; Fig. 2*D*).

Pharmacology of $\epsilon 2^{-/-}$ NMDA receptors is consistent with $\zeta 1/\epsilon 1$ receptors

Experiments using recombinant receptors have provided pharmacological tools that can be diagnostic for specific diheteromeric subunit combinations. We used glycine (Kutsuwada et al. 1992), Zn^{2+} (Paoletti et al. 1997), and ifenprodil (Williams 1993) to investigate the subunit composition of NMDA receptors from $\epsilon 2^{-/-}$ neurons.

Recombinant $\zeta 1/\epsilon 1$ receptors are more than tenfold less sensitive to glycine than $\zeta 1/\epsilon 2$ receptors (Kutsuwada et al. 1992). We measured the deactivation of whole cell glycine-evoked currents from $\epsilon 2^{-/-}$ and wild-type neurons (Fig. 3*A*) using fast application methods. Glycine deactivations from $\epsilon 2^{-/-}$ neurons decayed quickly and were well-fitted by single exponentials (0.11 ± 0.1 s, $n = 6$) whereas the deactivations from wild-type neurons were slower and required two exponential components to be well-fitted ($\tau_f = 0.266 \pm 0.2$ s, $\tau_s = 1.38 \pm 0.06$ s, $n = 6$). This is consistent with an eight- to tenfold faster glycine microscopic unbinding rate in receptors from $\epsilon 2^{-/-}$ neurons. We confirmed the lower glycine affinity of receptors from $\epsilon 2^{-/-}$ neurons by comparing the glycine dose-response relationship for $\epsilon 2^{-/-}$ ($EC_{50} = 3.61$ μM) with wild-type ($EC_{50} = 0.14$ μM) neurons (Fig. 3*A*). The EC_{50} value for $\epsilon 2^{-/-}$ NMDA receptors is consistent with that of $\zeta 1/\epsilon 1$-containing NMDA receptors (Kutsuwada et al. 1992).

Recombinant $\zeta 1/\epsilon 1$ receptors are also selectively antagonized in a voltage-independent manner by nanomolar Zn^{2+} (Paoletti et al. 1997). Because the IC_{50} for high-affinity Zn^{2+} antagonism is near the levels of contaminating Zn^{2+} (Paoletti et al. 1997), the high-affinity Zn^{2+} chelator TPEN (1 μM) was included in the control solution. Whole cell NMDA (1 mM) currents from wild-type neurons (Fig. 3*B*) were reduced slightly in Zn^{2+} (500 nM; 80.8 ± 3.0% of control, $n = 6$) whereas currents from neurons lacking $\epsilon 2$ were almost completely blocked (18.1 ± 1.8% of control, $n = 6$). In contrast, the selective $\zeta 1/\epsilon 2$ receptor antagonist ifenprodil (3 μM: Williams 1993) reduced whole cell NMDA (1 mM) currents from wild-type (33.3 ± 6.0% of control, $n = 8$) to a much greater extent than currents from $\epsilon 2^{-/-}$ neurons (85.2 ± 1.7%, $n = 5$; Fig. 3C). Thus the pharmacological profile of $\epsilon 2^{-/-}$ NMDA receptors is consistent with that expected from $\zeta 1/\epsilon 1$ heteromers.

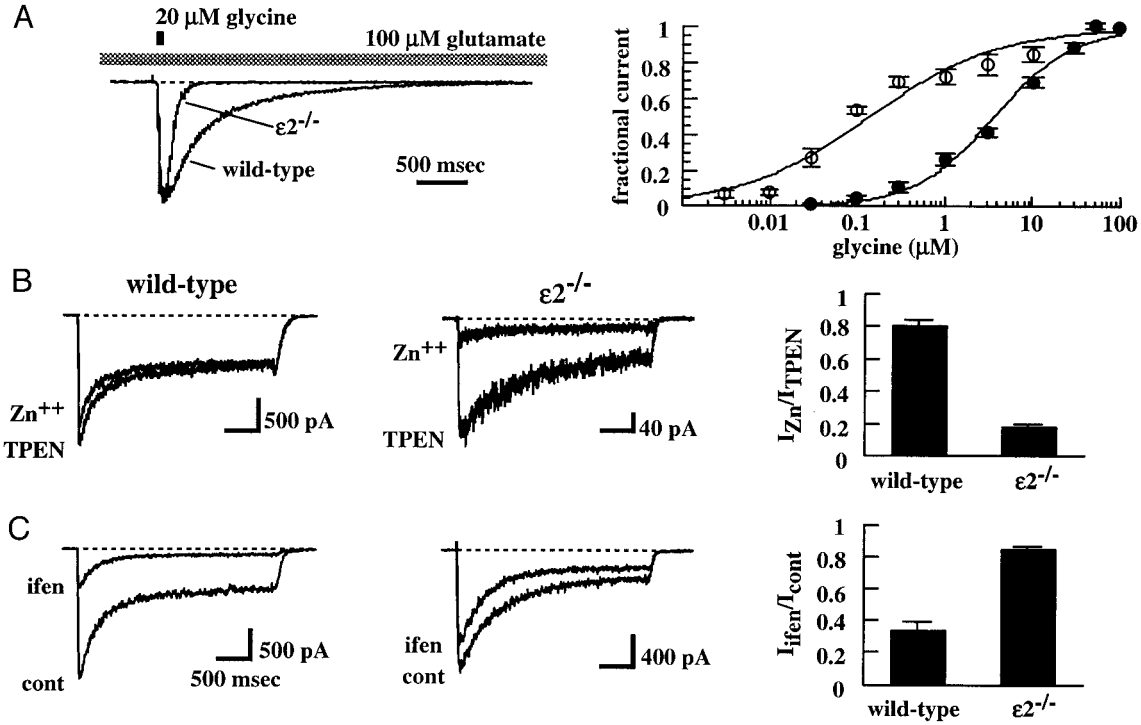

FIG. 3. The pharmacological characteristics of NMDA receptors from $\epsilon 2^{-/-}$ neurons are consistent with $\zeta 1/\epsilon 1$ receptors. *A* (*left*): deactivation time course of glycine-activated currents (20 μM, 100 ms) in the continuous presence of glutamate (100 μM) was much faster in neurons lacking $\epsilon 2^{-/-}$, consistent with a faster microscopic dissociation rate. Glycine deactivation kinetics were measured using calibration-grade glutamate. *A* (*right*): steady-state glycine dose-response curve for wild-type (○) and $\epsilon 2^{-/-}$ (●) neurons to NMDA applications. All responses were normalized to the response at 50 μM (wild-type) or 100 μM ($\epsilon 2^{-/-}$). From the logistic equation, the EC50 was 0.133 μM (wild-type) and 3.61 μM ($\epsilon 2^{-/-}$) with Hill coefficients of 0.80 (wild-type) and 0.97 ($\epsilon 2^{-/-}$). NMDA receptors from $\epsilon 2^{-/-}$ neurons were blocked by low concentrations of Zn^{2+} but much less sensitive to ifenprodil. *B*: wild-type (*left*) and $\epsilon 2^{-/-}$ currents (*center*) in the presence of 500 nM added Zn^{2+} or the high-affinity Zn^{2+} chelator TPEN. *C*: compared with wild-type currents (*left*), currents from $\epsilon 2^{-/-}$ neurons (*center*) were much less sensitive to ifenprodil (3 μM).

DISCUSSION

NMDA receptor–mediated EPSCs from cultured hippocampal neurons lacking the $\epsilon 2$ subunit have very fast deactivation kinetics compared with those from wild-type neurons. Fast NMDA receptor–mediated EPSC kinetics have been reported in wild-type animals but seem to be the exception rather than the norm. EPSC deactivation kinetics similar to those reported here occur during synapse formation in the rat spinal cord (Bardoni et al. 1998) and cerebellar granule cells (D'Angelo et al. 1993). Additionally, EPSC deactivation kinetics recorded from mature synapses on cerebellar granule neurons from mice lacking the $\epsilon 3$ (NR2C) subunit are very similar to those that we report from $\epsilon 2^{-/-}$ neurons (Ebralidze et al. 1996). NMDA receptor–mediated EPSC deactivation kinetics in other preparations are comparable to our results from wild-type neurons. The slow kinetics of the NMDA receptor–mediated EPSC have been thought to account for rhythmic, pacemaker activities like breathing, locomotion, and suckling, arising from central pattern generators in brainstem nuclei and the spinal cord. However, the neonatal death in mice lacking the $\epsilon 2$ subunit most likely results from the absence of synaptic NMDA receptors in regions otherwise expressing the $\epsilon 2$ subunit, rather than changes in deactivation kinetics.

Our data indicates that the $\epsilon 2$ subunit is not required for synaptic localization of NMDA receptors. Previous work with these animals reported a lack of the NMDA receptor–mediated component of the field EPSP in $\epsilon 2^{-/-}$ hippocampi from animals at postnatal day 2–3 (Kutsuwada et al. 1996). This is consistent with our observation that NMDA-evoked currents from $\epsilon 2^{-/-}$ neurons often do not appear until 4–5 DIV and $\epsilon 1$ is not expressed until after this time in vivo (Monyer et al. 1994; Sheng et al. 1994). The increase in expression of $\epsilon 1$ is coincident with the acceleration of the wild-type NMDA receptor–mediated deactivation kinetics (Carmingnoto and Vicini 1992; Hestrin 1992).

On the basis of the characteristics of NMDA receptor–mediated EPSCs, we propose that the NMDA receptors expressed in $\epsilon 2^{-/-}$ neurons are $\zeta 1/\epsilon 1$ diheteromeric receptors. If this is true, this means that the signals required for NMDA receptor targeting to the somato-dendritic membrane and/or synaptic localization of NMDA receptors are found on $\zeta 1$ or $\epsilon 1$. The $\epsilon 2$ subunit is required early in development because of a need for functional NMDA receptors rather than targeting (to the somato-dendritic membrane) or localization (to the postsynaptic membrane) of synaptic receptors. Targeting and localization events may require different amino acid sequence motifs. The carboxy-terminal intracellular regions of $\epsilon 1$ and $\epsilon 2$ have amino acid sequence homologies in the region just after the final transmembrane segment and at the PDZ recognition sites at the carboxy termini. Mice lacking the PDZ recognition sequences in $\epsilon 2$ show decreased levels of synaptic NMDA receptors (Mori et al. 1998). This suggests that NMDA receptor targeting is retained but synaptic localization may be reduced. Furthermore, proteins that bind to the PDZ domain such

as PSD-95 are not required for synaptic localization of these receptors. The AMPA receptor–mediated component appears normal in animals without the NMDA receptor–mediated component (Kutsuwada et al. 1996), indicating that incorporation of AMPA receptors at synapses is independent of NMDA receptor activation.

We thank Dr. Masayoshi Mishina for a gift of ε2-targeted mice and A. Miller for technical assistance with genotyping.

This work was supported by National Institute of Mental Health Grants MH-11204 to K. R. Tovar and MH-46613 to G. L. Westbrook. K. R. Tovar was also supported by the Scottish Rite Schizophrenia Research Program, Northern Masonic Jurisdiction, USA.

Address for reprint requests: G. L. Westbrook, Vollum Institute, L474, Oregon Health Sciences University, 3181 S. W. Sam Jackson Park Rd., Portland, OR 97201-3098.

Received 13 July 1999; accepted in final form 1 September 1999.

REFERENCES

BARDONI, R., MAGHERINI, P. C., AND MACDERMOTT, A. B. NMDA EPSCs at glutamatergic synapses in the spinal cord of the postnatal rat. *J Neurosci.* 18: 6558–6567, 1998.

BEKKERS, J. M. AND STEVENS, C. F. Excitatory and inhibitory autaptic currents in isolated hippocampal neurons maintained in cell culture. *Proc. Natl. Acad. Sci. USA* 88: 7834–7838, 1991.

CARMINGNOTO, G. AND VICINI, S. Activity-dependent decreases in NMDA receptor responses during development of the visual cortex. *Science* 258: 1007–1111, 1992.

D'ANGELO, E., ROSSI P., AND TAGLIETTI, V. Different proportions of *N*-methyl-D-aspartate and non-*N*-methyl-D-aspartate receptor currents at the mossy fibre-granule cell synapse of developing rat cerebellum. *Neuroscience* 53: 121–130, 1993.

DAS S., SASAKI, Y. F., ROTHE, T., PREMKUMAR, L. S., TAKASU, M., CRANDELL, J. E., DIKKES, P., CONNER, D. A., RAYUDU, P. V., CHEUNG, W., CHEN, H. S., LIPTON, S. A., AND NAKANISHI, N. Increased NMDA current and spine density in mice lacking the NMDA receptor subunit NR3A. *Nature* 393: 377–381, 1998.

EBRALIDZE, A. K., ROSSI, D. J., TONEGAWA, S., AND SLATER, N. T. Modification of NMDA receptor channels and synaptic transmission by targeted disruption of the NR2C gene. *J. Neurosci.* 15: 5014–5025, 1996.

HESTRIN, S. Developmental regulation of NMDA receptor–mediated synaptic currents at a central synapse. *Nature* 357: 686–689, 1992.

KUTSUWADA, T., KASHIWABUCHI. N., MORI. H., SAKIMURA, K., KUSHIYA, E., ARAKI, K., MEGURO, H., MASAKI, H., KUMANISHI, T., ARAKAWA, M., AND MISHINA, M. Molecular diversity of the NMDA receptor channel. *Nature* 358: 36–41, 1992.

KUTSUWADA, T., SAKIMURA, K., MANABE, T., TAKAYAMA, C., KATAKURA, N., KUSHIYA, E., NATSUME, R., WATANABE, M., INOUE, Y., YAGI, T., AIZAWA, S., ARAKAWA, M., TAKAHASHI, T., NAKAMURA, Y., MORI, H., AND MISHINA, M. Impairment of suckling response, trigeminal neuronal pattern formation, and hippocampal LTD in NMDA receptor ε2 subunit mutant mice. *Neuron* 16: 333–344, 1996.

LI, J. H., WANG, Y. H., WOLFE, B. B., KRUEGER, K. E., CORSI, L., STOCCA, G., AND VICINI, S. Developmental changes in localization of NMDA receptor subunits in primary cultures of cortical neurons. *Eur. J. Neurosci.* 10: 1704–1715, 1998.

MCBAIN, C. J. AND MAYER, M. L. NMDA receptor structure and function. *Physiol Rev.* 74: 723–760, 1994.

MONYER, H., BURNASHEV, N., LAURIE, D. J., SAKMANN, B., AND SEEBURG, P. H. Developmental and regional expression in the rat brain and functional properties of four NMDA receptors. *Neuron* 12: 529–540, 1994.

MORI, H., MANABE, T., WATANABE, M., SATOH, Y., SUZUKI, N., TOKI, S., NAKAMURA, K., YAGI, T., KUSHIYA, E., TAKAHASHI, T., INOUE, Y., SAKIMURA, K., AND MISHINA, M. Role of the carboxy-terminal region of the GluR ε2 subunit in synaptic localization of the NMDA receptor channel. *Neuron* 21: 571–580, 1998.

PAOLETTI, P., ASCHER, P., AND NEYTON, J. High-affinity zinc inhibition of NMDA NR1-NR2A receptors. *J. Neurosci.* 17: 5711–5725, 1997.

SAKIMURA, K., KUTSUWADA, T., ITO, I., MANABE, T., TAKAYAMA, C., KUSHIYA, E., YAGI, T., AIZAWA, S., INOUE, Y., SUGIYAMA, H., AND MISHINA, M. Reduced hippocampal LTP and spatial learning in mice lacking NMDA receptor ε1 subunit. *Nature* 373: 151–155, 1995.

SHENG, M., CUMMINGS, J., ROLDAN, L. A., JAN, Y. N., AND JAN, L. Y. Changing subunit composition of heteromeric NMDA receptors during development in rat cortex. *Nature* 368: 144–147, 1994.

SPRENGEL, R., SUCHANEK, B., AMICO, C., BRUSA, R., BURNASHEV, N., ROZOV, A., HVALBY, O., JENSEN, V., PAULSEN, O., ANDERSEN, P., KIM, J. J., THOMPSON, R. F., SUN, W., WEBSTER, L. C., GRANT, S. G., EILERS, J., KONNERTH, A., LI, J., MCNAMARA, J. O., AND SEEBURG, P. H. Importance of the intracellular domain of NR2 subunits for NMDA receptor function in vivo. *Cell* 92: 279–289, 1998.

STOCCA, G. AND VICINI, S. Increased contribution of NR2A subunit to synaptic NMDA receptors in developing rat cortical neurons. *J. Physiol. (Lond.)* 507: 13–24, 1998.

TOVAR, K. R. AND WESTBROOK, G. L. The incorporation of NMDA receptors with a distinct subunit composition at nascent hippocampal synapses in vitro. *J. Neurosci.* 19: 4180–4188, 1999.

VICINI, S., WANG, J., LI, J., ZHU, W., WANG, Y., LUO, J., WOLFE, B., AND GRAYSON, D. Functional and pharmacological differences between recombinant *N*-methyl-D-aspartate receptors. *J. Neurophysiol.* 79: 555–566, 1998.

WILLIAMS, K. Ifenprodil discriminates subtypes of the *N*-methyl-D-aspartate receptor: selectivity and mechanisms at recombinant heteromeric receptors. *Mol. Pharm.* 44: 851–859, 1993.